Long-term variations in palaeointensity

Peter A. Selkin and Lisa Tauxe

Phil. Trans. R. Soc. Lond. A 2000 **358**, 1065-1088
doi: 10.1098/rsta.2000.0574

Long-term variations in palaeointensity

By Peter A. Selkin and Lisa Tauxe

Scripps Institution of Oceanography, University of California at San Diego, Mail Code 0220, La Jolla, CA 92037-0220, USA

We compile a dataset of reliable palaeointensity estimates based both on published work and on new data from basaltic glass. The basaltic glass data more than double the number of reliable (Thellier method with pTRM checks) palaeointensity estimates available. Although the new data dramatically improve both spatial and temporal coverage, there is still a strong bias toward the most recent past. The last 0.3 Ma claim over half of the data in our combined database. We therefore divide the data into two groups, the densely sampled last 0.3 Myr and the more sparsely sampled period of time comprising roughly half of the data from 0.3 to 300 Ma. Separating them in this way, it is clear that the dipole moment of the Earth over the past 0.3 Myr (*ca.* 8×10^{22} A m^2) is dramatically higher than the average dipole moment over the preceding 300 Myr (*ca.* 5×10^{22} A m^2). Inclusion of poor-quality results leads to an overestimate of the average dipole moment. Interestingly, no other significant changes in the distribution of dipole moments are evident over the 300 million year span of the data.

Keywords: palaeointensity; palaeomagnetism; submarine basaltic glass; Thelliers' method

1. Introduction

Of the parts of Earth's layered structure, the core remains the least well understood. One can study its evolution through time by examining variations in the geomagnetic field. Though by nature indirect (it assumes that the present inferred connection between outer-core convection and the geomagnetic field has always operated in the past), it is a relatively more direct way of studying the evolution of the core than those provided by other fields such as geochemistry and meteoritics. Any convincing explanation of the geomagnetic field's variation through time must be based on a high-quality global dataset. To this end, a number of groups worldwide are currently developing high-resolution and/or long-term global palaeomagnetic databases (see, for example, Perrin & Scherbakov 1997). In the near future, the geomagnetic community hopes to interpret these datasets in terms of outer-core dynamics. Such an interpretation is not yet within our grasp (and is certainly too ambitious for this article). Indeed, because of the sparsity of the data in space and in time, and because of differences in technique and acceptability criteria among laboratories, it is difficult—though by no means impossible—even to discern significant long-term trends in the palaeomagnetic data.

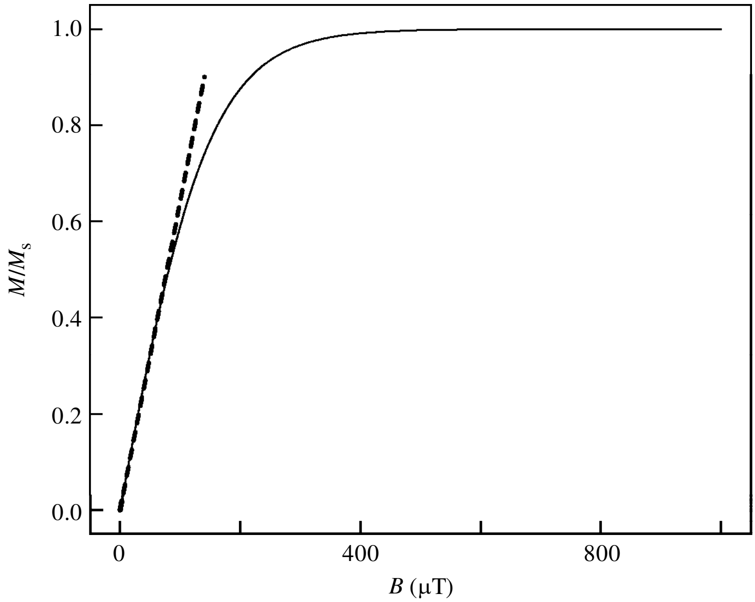

Figure 1. An example of thermal remanence acquisition as a function of applied field B for magnetite, as predicted by single-domain theory. M/M_s is the magnetization as a fraction of saturation acquired at a blocking temperature (T) of 300 °C, using Boltzmann's constant k. Particles are assumed to be single domain and non-interacting with a grain diameter d of 50 nm with volume v of d^3. The heavy dashed line is the approximation of linearity with applied field, which breaks down at *ca.* 120 μT. TRM approaches saturation above *ca.* 200 μT, so no palaeointensity estimates are possible above about this field strength.

2. Palaeointensity methods

(*a*) *A comparison of palaeointensity techniques*

(i) *Theoretical basis*

Techniques for estimating absolute palaeointensity are based on a simple idea: that a population of magnetic particles, when cooled below their blocking temperature, will become magnetized in proportion to the ambient magnetic field if the field is relatively weak. For the size ranges of magnetic mineral grains in palaeomagnetic and archaeomagnetic specimens, the geomagnetic field qualifies as 'relatively weak'.

The exact ratio of the applied field to the magnetization of the sample cannot be predicted *a priori*. The single-domain theory of Néel (1949) does predict a hyperbolic tangent relationship between the thermoremanent magnetization (TRM) of an assemblage of single-domain magnetic particles and an applied magnetic field. For weak applied fields, this relationship is approximately linear (for example, see figure 1). Single-domain theory, however, applies only to a population of non-interacting single-domain grains. The magnetic particles in such an ensemble must all have the same volume and must all have the same blocking temperature. Because natural materials typically have a range of grain sizes and blocking temperatures, single-domain theory cannot accurately predict their thermoremanent magnetization.

Early studies (see Thellier & Thellier 1959) determined empirically the relationship between an artificial TRM (M_{TRM}) acquired in a laboratory field (B_{lab}) and the intensity of that laboratory field. They then used the following relationship to estimate the intensity of the magnetic field (B_{ancient}) in which their samples acquired a natural TRM (M_{NRM}):

$$B_{\mathrm{ancient}} = B_{\mathrm{lab}} \frac{M_{\mathrm{NRM}}}{M_{\mathrm{TRM}}}. \tag{2.1}$$

The above equation suggests a simple and straightforward palaeointensity experiment. However, it is based on the assumption that a particle demagnetized by heating above its blocking temperature becomes thermally remagnetized when cooled below that same temperature in an applied field. If blocking and unblocking temperatures were identical, the experiments described above would suffice. In geological samples, however, magnetic particles may be altered to other minerals with different magnetic properties. Geological samples may also contain multidomain grains, in which the blocking and unblocking temperatures may not be the same. The ensemble of magnetic particles in a sample may change drastically when the sample is heated, especially to the high unblocking temperatures typical of magnetite and haematite. Furthermore, populations of magnetic minerals may acquire a viscous overprint after being thermally magnetized.

(ii) *Method of Thellier & Thellier (1959)*

Palaeomagnetists have devised a variety of techniques to circumvent the problems of alteration, viscous overprinting and multidomain behaviour. The most rigorous of these was developed by E. & O. Thellier (1959). A Thellier–Thellier-type experiment is based on the assumption that magnetic particles in rocks come in a range of sizes. Each volume fraction will become superparamagnetic above a different blocking temperature. These particles will thus lose their remanent magnetization (or gain an artificial TRM) at some unblocking (or blocking) temperature lower than the maximum unblocking temperature for the entire sample.

The experiment itself consists of a series of double-heating steps, each of which involves two measurements of the sample's magnetic moment. One first measures the portion of a sample's natural remanent magnetization that remains after heating to some temperature and cooling in a known, and typically null, field. The sample is then reheated to the same temperature and cooled in a magnetic field, roughly comparable in intensity to the expected ancient field, and its moment remeasured (the moment gained is termed partial TRM, or pTRM). To simplify analysis of the NRM–pTRM data, the fields used to impart the pTRMs should be in the same orientation relative to the sample. The process is repeated at progressively higher temperatures up to the sample's maximum unblocking temperature. The Thelliers' double-heating method has one clear advantage over single-step methods: heating in steps allows one to identify temperature ranges over which the relationship between NRM and TRM does not change. This suggests, but does not prove, that the sample is not being altered over this range of temperatures.

A modification of the Thellier experiment was proposed by Wilson (1961), who heated and cooled a sample multiple times in a range of applied fields at each temperature step. This method has not been used frequently since Wilson's study, presumably because of the amount of time required for each multiple-heating step. Except when used with strong fields for which the Néel relationship in figure 1 is strongly nonlinear, the Wilson method reveals no more about the sample's acquisition of TRM than does the Thellier experiment.

A more sensitive test for alteration at any particular step is the method of pTRM checks. Suggested by Thellier & Thellier (1959) and discussed at length by Coe (1967), this method involves repeating a previous in-field step after a higher temperature zero-field step. If the sample's magnetic mineralogy has only changed reversibly, the pTRM gained during the pTRM check will be the same as that gained in the double-heating step which it repeats. This is the only method that allows the experimenter to check for irreversible changes in a sample's magnetic moment while the experiment is in progress. It is also the only method which allows the experimenter to base a palaeointensity estimate on a portion of the demagnetization–remagnetization data from a sample.

(iii) *Other methods: Shaw and Van Zijl*

Besides the Thelliers' technique, several other types of palaeointensity experiments have been proposed. In particular, the methods of Shaw (1974; modified by Kono 1978 and Rolph & Shaw 1985) and of Van Zijl *et al*. (1962) are in common use. In Shaw's method, the palaeointensity estimate is based on a portion of the sample's coercivity spectrum—as opposed to a portion of the sample's blocking temperature spectrum, as in the Thelliers' procedure. The procedure involves stepwise demagnetization of a sample four separate times in an alternating field. The first demagnetization yields the coercivity spectrum of the sample's initial NRM. The sample is then given an anhysteric remanent magnetization (ARM), a single-temperature total or nearly total TRM, and another ARM, each of which is demagnetized in step-wise alternating fields. The intensity of the bias field used to produce the ARM does not need to be the same as that of the field imposed during the TRM step, although the DC fields of the two ARMs must be of the same magnitude. One then compares the coercivity spectra of the two ARMs, and, in the original Shaw method, selects a portion of the coercivity spectrum over which the ratio between the two is unity. Shaw (1974) argues that the particles represented by these coercivities have not altered during the experiment. The NRM and TRM are then compared over those same coercivities. In the modified Shaw procedure, AF demagnetization steps for which ARM2/ARM1 is not equal to unity are corrected: the ratio of NRM to TRM for each of those coercivities is multiplied by ARM2/ARM1 for the same coercivity.

The experiments of Van Zijl *et al*. (1962) are similar to Shaw's in that they involve demagnetizing a specimen's NRM and TRM in an alternating field. The Van Zijl method partly demagnetizes the specimen's NRM in an alternating field, imposes a TRM on that sample and demagnetizes that in an alternating field. The peak intensities of the two alternating fields must be identical. The ratio of partly demagnetized TRM to partly demagnetized NRM is used to determine the palaeointensity. Partly demagnetizing the samples in alternating fields will reduce the effects of viscous remagnetization.

Neither the Shaw method—in its original or modified forms—nor the Van Zijl method test for alteration or for other irreversible magnetic behaviour while the sample is being heated. Goguitchaichvili *et al*. (1999) have retested, using a modified Thellier procedure, some palaeointensity estimates originally made using the

Shaw method. The two methods imply different estimated palaeointensities. Thermomagnetic (susceptibility–temperature) tests indicated that heating the samples to high temperatures had probably altered the magnetic mineralogy. Such a change is apparent in a Thellier experiment—especially in one that uses pTRM checks—but would not necessarily be obvious in an experiment that does not measure NRM–pTRM changes during heating. Methods that do check accurately for irreversible magnetic behaviour during heating will likely reduce the variance within a set of palaeointensity estimates from the same site (i.e. for a set of samples that have acquired a natural TRM in the same palaeofield).

(*b*) *The quality of palaeointensity estimates*

In spite of the modified Thellier experiment's rigour, it is still not a trivial process to choose the correct portion of the blocking temperature spectrum on which to base a palaeointensity estimate. Coe *et al*. (1978) propose a 'quality factor' (q) for Thellier-method palaeointensity estimates. This statistic takes into account the relative uncertainty in the ratio NRM/TRM determined at different temperature steps, the fraction of the NRM lost over the selected demagnetization steps and the average NRM lost between steps in the selected interval.

There is even more information in a modified Thellier experiment than can be encapsulated in the quality factor. Coe *et al*. (1978) did not base their temperature-range selection on q alone: they require that pTRM checks be positive and that the NRM demagnetized over the selected temperatures be a primary TRM. Pick & Tauxe (1993*a*) suggested that a further requirement should be that the NRM vector for the selected temperature interval trends toward the origin on a vector endpoint diagram. We have developed a set of strict criteria, based on those of Coe *et al*. and Pick & Tauxe (1993*a*), which we apply in this study to data from all Thellier experiments performed at Scripps on submarine basaltic glass. We include new data from basaltic glasses in the Ocean Drilling Program core collection (see below). The data from each submarine basaltic glass specimen have been reanalysed using the following set of criteria.

(1) The Thellier method and its variants assume that the zero-field steps demagnetize an igneous-rock sample's primary TRM. To determine whether this is true, we plot the zero-field steps as a vector endpoint diagram in sample coordinates. The Z-axis of this coordinate system corresponds to the axis of our cylindrical samples and to the direction of the laboratory field applied in the in-field cooling steps. The X-axis corresponds to an arbitrary fiducial arrow marked on the top of each cylindrical pellet. The data are plotted (e.g. figure 2*a*–*e*) with X–Y data pairs as solid symbols and X–Z pairs as open symbols. We calculate the principal component of the data points corresponding to the chosen temperature range using the method of Kirschvink (1980). The principal component of these data should trend toward the origin if the points represent the primary component of the NRM (and not a viscous overprint or some component of unknown origin). We compare the vector average of the selected data with the principal component. The former is anchored to the origin, whereas the latter, shown in figure 2*a*(i), for example, as a dashed line, is anchored to the centre of mass of the data. The angle (α) between these two vectors must be less

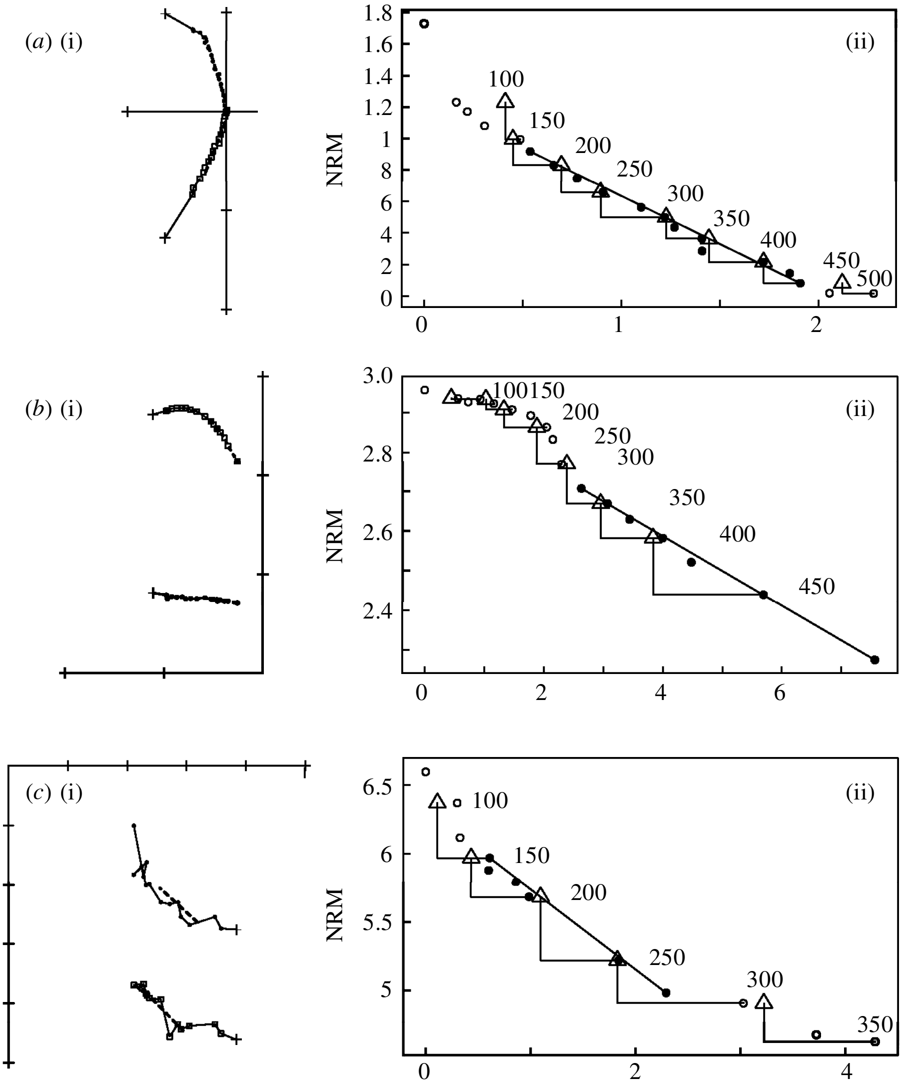

Figure 2. (a)–(e)(i) Vector endpoint diagrams of the magnetization remaining after each cooling in zero field. Specimens are unoriented, but the vertical axis (Z) is the direction along which the laboratory field was applied during pTRM acquisition. Solid symbols are X–Y pairs and open symbols are X–Z pairs, where X is an arbitrary direction perpendicular to Z. (a)–(e)(ii) Arai plots of the specimens shown in (a)–(e)(i). These are pTRM gained after cooling in a laboratory field versus NRM remaining after cooling in zero field. Solid symbols indicate the points used in the calculation of palaeointensity. Triangles are the pTRM checks. (a) Specimen passing all criteria for acceptance. Units are 10^{-8} A m^2. (b) Specimen that fails the α criterion, but passes all others. Units are 10^{-8} A m^2 on the NRM and 10^{-9} A m^2 on the pTRM axis. (c) Specimen that fails the MAD criterion, but passes all others. Units are 10^{-10} A m^2. (d) Specimen that fails the β criterion, but passes all others. Units are 10^{-9} A m^2. (e) Specimen that fails the DRAT criterion, but passes all others. Units are 10^{-8} A m^2.

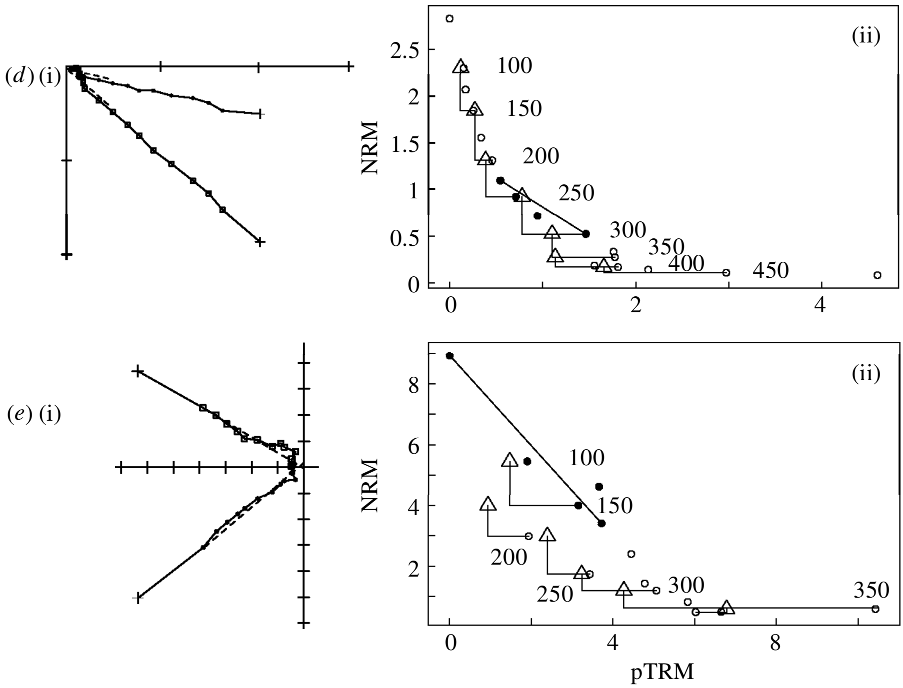

Figure 2. (*Cont.*)

than 15°. The selected points in figure 2*a* trend to the origin, whereas those in figure 2*b* do not.

(2) We wish to insure that one and only one component of the NRM is demagnetized in the selected zero-field steps. To this end we calculate the maximum angular deviation (MAD; Kirschvink 1980) along with the principal component. The MAD is a qualitative indication of scatter about the principal component. A maximum value of MAD was taken to be 15°. The MAD for the selected data shown in figure 2*c* exceeds the MAD criterion.

(3) The data are plotted on an 'Arai plot' (Nagata *et al.* 1963) as NRM remaining versus pTRM gained in each temperature step (figure 2(*a*)–(*e*)(ii)). We calculate a best-fit line to groups of four or more data points by the method of Coe *et al.* (1978). The latter use the ratio of the standard error of the slope (σ) to the absolute value of the slope ($|b|$) to describe the relative uncertainty in the slope of that best-fit line and thus the relative uncertainty in the palaeointensity estimate. We call this statistic β. Based on visual inspection of many Arai plots, we chose an arbitrary value of $\beta = 0.1$ as a maximum acceptable scatter. The data shown in figure 2*d*(ii) fail this criterion.

(4) Failure of a pTRM check is an indication of either poor reproducibility (usually accompanied by large scatter) or of irreversible changes in the ferromagnetic minerals in the specimen. We calculate the difference between the two in-field measurements for a given pTRM check. It is common practice to require two in-field measurements at the same temperature to agree to within 5% (see,

PHILOSOPHICAL TRANSACTIONS OF THE ROYAL SOCIETY A MATHEMATICAL, PHYSICAL & ENGINEERING SCIENCES

for example, Pick & Tauxe 1993*a*, *b* 1994). This test has a bias against the lower-temperature steps: the pTRM acquired in those steps is rather small, so reproducibility to a given percentage is more difficult to achieve. Here, we take a somewhat different approach that instead penalizes those field estimates which are based on a small fraction of the NRM. We normalize the difference between repeat pTRM steps by the length of the selected NRM–pTRM segment and express the difference ratio (DRAT) as a percentage. A DRAT of 10% is the maximum acceptable value for our DRAT criterion. The data shown in figure 2*e*(ii) fail the DRAT criterion.

(5) In addition to the aforementioned criteria, we reject points with q values of less than unity. Though lenient and redundant in most cases, this constraint is necessary to make certain that our palaeointensity estimates are not based on an inordinately small fraction of the NRM. Consider four NRM–pTRM points which meet the rest of our criteria. If the NRMs are equally spaced on an Arai plot (the 'gap factor' of Coe *et al*. (1978) is $\frac{2}{3}$) and $q = 1$, only 15% of the NRM is demagnetized over the selected temperature range. Samples with even lower q values are thus based on a dangerously small portion of the NRM–pTRM data.

(6) In situations in which more than one specimen from the same sampling location passes our previous criteria, we average the field estimates (B) from both or all specimens. If the ratio of the standard deviation of the field estimates to the average ($\sigma_B/\bar{B}$) is greater than 25%, we deem the average unreliable and do not consider it in further calculations.

(*c*) *Submarine basaltic glass samples*

Previous work has shown that the glassy rinds of submarine pillow basalts and sheet flows are excellent materials for palaeointensity experiments (see, for example, Pick & Tauxe 1993*a*, 1994). Rock magnetic studies suggest that low-Ti single-domain titanomagnetite carries the remanent magnetization in these samples (Pick & Tauxe 1994). Furthermore, the remanence is acquired on time-scales comparable with laboratory cooling times. Thus the material satisfies many of the assumptions behind the Thellier experiment. In fresh samples, the remanence is likely a TRM acquired when the glass cooled almost immediately after eruption. Modified Thellier experiments on basaltic glass from the site of a recent eruption recover the present field at that location (Pick & Tauxe 1993*a*). Because the ocean basins cover a large area of the Earth's surface, and because the age of the sea floor in many places is well constrained, submarine basaltic glass is a great resource for studies of palaeointensity. Researchers at the Scripps Institution of Oceanography's palaeomagnetic laboratory have contributed a large volume of palaeointensity estimates since work began on the project in 1993 (see, for example, Pick & Tauxe 1993*a*, *b*, 1994; Juarez *et al*. 1998; Juarez & Tauxe 2000).

The new specimens used in this study were taken from Ocean Drilling Program (ODP) cores. Samples were taken from all available ODP cores wherever glass was noted in core descriptions. These bulk samples (of the order of 5–10 g of rock) were then sorted by degree of alteration. The latter was determined based on the colour and lustre of the rock samples. The freshest pieces were broken into chips of *ca.* 0.1–0.5 g each. Care was taken to choose the freshest looking glass possible, free of palagonite, large mineral grains, dirt or sparry calcite. In some cases, the glassy rind of a pillow was so thin that samples could not be separated from the underlying basalt. We tried to minimize the amount of basalt attached to the glass. The chips were cleaned in HCl if any calcite, clay or other contaminant was noted; all chips were then washed with deionized water.

Chips of basaltic glass that had too low a magnetic moment (less than or equal to 0.5 nA m^2) were rejected. The rest of the chips were pressed into NaCl pellets, which were then scribed with a fiducial mark so that they could be oriented throughout the experiment. The pellets were then subjected to a stepwise double-heating experiment modified after the method of Thellier & Thellier (1959; modifications of Coe *et al.* 1978). Temperature steps began at 100° and proceeded at 25° increments until the specimen began to fail our criteria mentioned above or until the specimen had lost *ca.* 90% of its remanence. At every other double-heating step (in 50° increments) we performed a pTRM check, heating the sample to 50° below the temperature used in the zero-field part of the step.

(*d*) *Starting dataset for analysis of long-term trends*

We combine two databases to produce a palaeointensity dataset spanning a long time period and covering as much of the Earth's surface as possible. The first is a database, available on the Internet at

ftp://ftp.dstu.univ-montp2.fr/pub/palaeointdb/pint.mdb .

We will refer to that database as PINT99 in the following. PINT99 comprises 1592 published absolute palaeointensity estimates. The editors of PINT99 accept palaeointensity estimates made by all techniques, from a wide range of locations and ages, and of any polarity. It is the current version of the database originally compiled by Tanaka *et al.* (1995) and more recently updated by Perrin & Scherbakov (1997) and Perrin *et al.* (1998). The second database we consider, the Scripps submarine basaltic glass (SBG99) database, contains 287 palaeointensity estimates from modified Thellier experiments on ODP, DSDP and ophiolitic submarine basaltic glass. Only palaeointensity estimates that passed the criteria listed above were included in SBG99.

We are combining data from two databases that contain the results of a wide range of experiments, all of different types and of varying degrees of reproducibility. To produce a reliable analysis of long-term trends in palaeointensity, we must start with a reliable dataset. To this end, we chose data from the PINT99 database based on the following.

(1) The Thellier palaeointensity method with pTRM checks is the only technique that provides robust palaeointensity estimates, uncontaminated by alteration or other irreversible changes in magnetic mineralogy. Therefore only palaeointensities estimated using the Thelliers' method and pTRM checks were accepted.

(2) Previous studies (see, for example, Prévot *et al.* 1985) have suggested that the geomagnetic field during polarity transitions is anomalously weak when

Table 1. *Locations, ages and average palaeointensities for DSDP/ODP glasses*

(Ages based on magnetic anomalies were determined using Cande & Kent (1995) or Harland *et al.* (1989) for M-series anomalies. Ages based on biostratigraphy were tied to the geomagnetic polarity timescale by Berggren *et al.* 1985*a*, *b*. Other references: CPC91, Castillo *et al.* (1991); JTGP98, Juarez *et al.* (1998); LL95, Lee & Lawver (1995); MRL93, Mueller *et al.* (1993); MSDSP93, Mahoney *et al.* (1993); PT93, Pick & Tauxe (1993*b*); V93, Van der Voo (1993); WS92*a*, Wallick & Steiner (1992*a*); WS92*b*, Wallick & Steiner (1992*b*); YK93, Yan & Kroenke (1993); IR136, Dziewonski *et al.* (1991); IR165, Sigurdsson *et al.* (1996); SR141, Forsythe *et al.* (1995); SR142, Goldstein *et al.* (1995).)

Site	plate	λ/ϕ	age (Ma)	method	λ'	method	B (μT)	N	σ	VADM
205	IN	−25/178	31 ± 1	C12N	−36	MRL93	16	4	3.6	2.85
238 (U)	IN	−11/71	34 ± 4	C11–C13	−24	MRL93	33	3	9.6	6.98
238 (L)	IN	−11/71	34 ± 4	C11–C13	−24	MRL93	9	3	0.0	1.90
322	AN	−60/−79	49 ± 1	C21–C22	−61	MRL93	28	4	6.1	3.99
332	NA	37/−34	3.9 ± 0.3	C2A	37	N/A	20	4	5.3	3.58
334	NA	37/−34	10.3 ± 0.1	C5N	36	MRL93	30	1		5.44
335	NA	37/−35	13.8 ± 1.3	C5A–C5B	37	MRL93	16	7	7.3	2.79
395	AF	23/−46	8 ± 1	C4N	23	MRL93	14	9	8.1	2.97
396	AF	23/−44	10.3 ± 0.5	C5N	23	MRL93	13	4	3.9	2.68
407	NA	64/−31	35.2 ± 0.3	C15R	60	MRL93	28	4	10.6	3.98
410	NA	46/−30	10.3 ± 0.7	C5N	45	MRL93	9	4	2.4	1.51
417	NA	25/−38	125 ± 1	M0	17	PT93	11	6	3.3	2.58
418	NA	25/−38	125 ± 1	M0	17	PT93	17	6	8.3	3.88
420	PA	9/−106	3.4 ± 0.2	C2A	9	N/A	14	3	3.5	3.58
423	PA	9/−105	1.7 ± 0.2	C2	9	N/A	12	3	1.5	2.91
447	PH	18/133	43.5 ± 5.5	C18–C21	10	LL95	21	2	14.8	5.08
448	PH	16/134	31 ± 2	NP23	9	LL95	18	1		4.49
462	NU	7/165	111 ± 1	CPC91	−33	S81	14	3	7.0	2.57
469	NA	33/−121	20 ± 2	C5E	35	MRL93	15	1		2.66
470	NA	29/−118	15.7 ± 0.7	C5B	24	MRL93	35	2	7.1	7.40
474	NA	23/−109	3.1 ± 0.2	C2A	23	N/A	22	9	4.1	4.66
482	NA	23/−108	0.3 ± 0.3	BRUNHES	23	N/A	24	2	15.6	5.14
483	NA	23/−108	2 ± 0.2	C2–C2A	23	N/A	29	16	17.1	6.12
495	CO	12.5/−91	22 ± 2	C6	2	JTGP98	18	5	2.5	4.59

Table 1. *Cont.*

Site	plate	λ/ϕ	age (Ma)	method	λ'	method	B (μT)	N	σ	VADM
504	NZ	1/−84	6.4 ± 0.2	C3A	1	N/A	10	3	6.6	2.58
510	CO	2/−86	2 ± 0.2	C2A	2	N/A	19	1		4.90
520	AF	−26/−11	14.9 ± 0.2	C5BR	−26	MRL93	19	2	16.3	3.81
522	AF	−27/−5	35.7 ± 1.3	C16	−30	MRL93	21	1		4.11
525	AF	−29/3	72 ± 1	C32N	−38	MRL93	55	8	6.6	9.66
534	NA	28/−75	156.5 ± 0.1	M28	9	V93	13	1		3.24
543	NA	16/−60	84 ± 1	C34(Y)	−21	PT93	7	3	2.1	1.46
556	NA	39/−35	32 ± 1.1	C12	36	MRL93	10	2	3.2	1.86
559	NA	35/−41	32 ± 1.1	C12	32	MRL93	11	2	0.7	2.00
562	NA	33/−42	17.9 ± 0.4	C5DR	32	MRL93	14	8	3.0	2.62
563	NA	34/−44	33.3 ± 0.3	C13	31	MRL93	18	2	0.7	3.38
564	NA	34/−44	33.3 ± 0.3	C13	31	MRL93	18	4	2.2	3.52
706	AF	−13/61	33.3 ± 0.2	C13	−19	MRL93	8	8	2.5	1.84
758	IN	5/90	78.3 ± 4.7	C33N–C34N	−54	MRL93	49	10	37.3	7.36
765	AU	−16/118	155.7 ± 0.3	M26	−32	V93	16	20	19.2	3.11
770	SA	5/124	38.9 ± 2.3	NP17	7	LL95	18	12	7.6	4.59
781	PH	20/147	1.68 ± 0.9	MATU.	20	N/A	40	1		8.90
801	PA	19/156	166.8 ± 4.5	CPC91	−9	WS92*b*	3	1		0.75
802	PA	12/153	114.6 ± 3.2	CPC91	−19.4	WS92*a*	20	1		4.37
803	OJP	2/161	88 ± 6	MSDSP93	−32	YK93	26	3	13.5	4.89
807	OJP	4/157	122.4 ± 0.8	MSDSP93	−34	YK93	26	39	13.2	4.74
834	IN	−19/−178	5.4 ± 0.2	N18	−19	N/A	12	5	2	2.72
835	IN	−19/−177	3.9 ± 0.5	CN11	−19	N/A	10	1		2.26
836	IN	−20/−177	1.0 ± 0.1	JARA.	−20	N/A	27	2	27	6.07
843	PA	19/−159	97 ± 5	CC9	−16	IR136	29	1		6.85
862	NZ	−47/−76	1.5 ± 0.1	SR141	−47	N/A	15	2	1.2	2.41
864	CO	10/−104	0.4 ± 0.3	SR142	10	N/A	38	7	4.2	9.45
907	EU	69/13	23 ± 0.4	C6B	57	V93	13	7	3.4	1.92
1001	CB	16/−76	77.6 ± 3.8	CC21	17	IR165	18	9	9	4.20

compared with long-term palaeointensity averages. Because palaeomagnetists have long focused on studying transitional palaeointensities, the database may be biased toward transitional records. To avoid bias, we reject data points designated as 'transitional' in the Montpellier database.

(3) For data based on averages of multiple specimens, we select points based on reproducibility. We express the ratio of the standard deviation (σ_B) to the mean of the set of measurements ($\bar{B}$) as a percentage, and reject points with $\sigma_B/\bar{B} \times 100$ (dF/F in PINT99) greater than 25%.

(4) To compare data from different locations, we calculate the virtual axial dipole moment (VADM) for each palaeofield estimate. The VADM associated with a palaeointensity estimate is the moment of the geocentric axial dipole that would produce a field of the specified palaeointensity at the sample's palaeolocation. The intensity of the present axial dipole of the geomagnetic field ranges from *ca.* 30 μT at the Equator to 60 μT at the poles. The VADM, however, evaluated anywhere on the Earth is 8×10^{22} A m^2.

To calculate a VADM from a palaeointensity estimate B_{ancient}, we use the following formula:

$$\text{VADM} = \frac{4\pi r_{\text{e}}^3}{\mu_0} B_{\text{ancient}} (1 + 3\cos^2\theta_{\text{s}})^{-1/2}. \quad (2.2)$$

In the above equation, r_{e} is the radius of the Earth, μ_0 the permeability of free space ($4\pi \times 10^{-7}$ Hm^{-1}), and θ_{s} the palaeocolatitude of the site. We therefore need to know the palaeolatitude of the site sampled. Had we decided instead to use virtual dipole moments (VDMs) which other authors (see, for example, Perrin & Scherbakov 1997) calculate instead of VADMs, we would need to know the magnetic palaeolatitude. Although geographic and magnetic palaeolatitudes are not often different by a large amount, magnetic palaeolatitudes require a large amount of high-quality directional data, which are not available for many sites. For sites younger than about 130 Ma, geographic palaeolatitudes can be calculated more consistently using plate reconstructions. We therefore calculate VADMs as opposed to VDMs in this study.

For the PINT99 and SBG99 databases, we list the method by which we determined the palaeolatitude along with other pertinent information about the sampling sites in table 1. Because plate motions over the past 5 Myr have not changed site latitudes enough to have a large effect on VADM calculations, we have used present latitudes to approximate the palaeolatitudes of all sites younger than 5 Ma. For sites younger than 130 Ma on the North American, South American, African, Australian–Indian and Antarctic plates, we calculated palaeolatitudes based on the fixed-hotspot model of Mueller *et al.* (1993). For sites older than 130 Ma on those plates as well as for sites from the Eurasian plate, we calculated palaeolatitudes (in strict terms, magnetic palaeolatitudes) from the apparent polar wander paths of Van der Voo (1993). For sites sampling Pacific crust younger than 40 Ma, we approximated the latitudinal component of plate velocity by a constant 0.4 deg Myr^{-1} northward. For all other sites, we relied on palaeogeographic reconstructions (Yan & Kroenke (1993) for old Pacific crust; Lee & Lawver (1995) for Southeast Asian microplates) or other pertinent data (e.g. palaeomagnetic inclinations from ODP holes 801 and 802 from Wallick & Steiner 1992*a*, *b*).

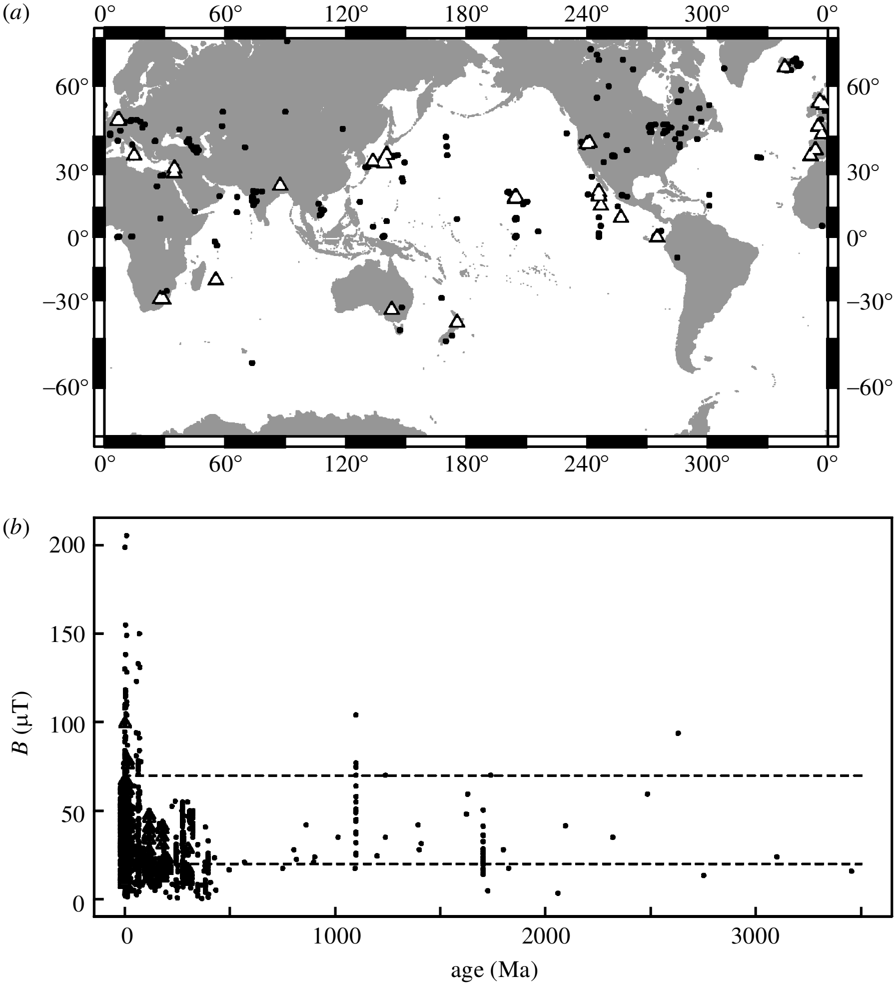

Figure 3. (*a*) Map of data from the PINT99 database. Dots (triangles) are data that are rejected (accepted) using the criteria discussed in the text. (*b*) Inferred values for B in the PINT99 database. Dots (triangles) are those rejected (accepted) for use in this paper. The dashed lines are the maximum and minimum values of the present field.

3. Analysis of long-term trends

(*a*) *Qualitative analysis of trends*

The results of applying our selection criteria to the PINT99 database are summarized in figure 3*a*, *b*. Applying the criteria to the PINT99 database pared the dataset down to a meagre 268 points out of 1592. The remaining points are restricted to the past 300 million years. The period from 15.5 to 93.5 Ma—which includes the entire Palaeogene—is entirely devoid of data, as is the period from *ca.* 201–290 Ma. In addition, sampling heavily favours mid-latitude sites.

The reduced dataset contains far fewer of the extremely high estimates of palaeointensity, many of which were based on Shaw-method experiments. We will evaluate this statistically in § 3 *b* (iii). The $\sigma_B/\bar{B} \times 100$ selection criterion removes many of the

PINT99 data points based on both Shaw and modified Thellier methods, eliminating roughly half of these points that satisfy the other criteria.

The new submarine basaltic glass dataset more than doubles the number of high-quality data available, adding 287 new palaeointensity estimates. The SBG99 database contains many points that fit in the widest gaps between surviving PINT99 data, including a large number of points from the early Tertiary and late Cretaceous. SBG99 contains data from two high-latitude sites as well, although the vast majority of the sites are at middle to low latitudes (see figure 4*a*).

Approximately 64% of the samples in the combined dataset (figure 4*b*) are Neogene or younger in age, *ca.* 23 Ma. This period is densely sampled, with an average of 13 samples per million years (compared with approximately 1.5 samples per million years for the dataset as a whole). When averaging the dataset, we must take care not to bias the average VADMs in favour of the present dipole moment. We will consider this point in more detail in § 3 *b* (i).

Some general features of the combined dataset bear mentioning. First, the VADM estimates from the combined dataset scatter widely about an average of 5.4×10^{22} A m^2 ($\sigma = 3.6 \times 10^{22}$ A m^2). The average VADM of the combined dataset is lower than the present dipole moment (*ca.* 8×10^{22} A m^2). Second, large virtual axial dipole moments are more common in the most recent data. This is particularly evident in figure 4*b*: the most recent VADMs are as high as 16×10^{22} A m^2, whereas VADMs above 8×10^{22} A m^2 are rare throughout the rest of the database.

(*b*) *Statistical analysis*

(i) *Temporal averages*

The recent period of high palaeointensity follows a period of low estimated VADM. However, samples from within the recent palaeointensity high are abundant in the database. In a histogram showing the age distribution (figure 5*a*) this is apparent as a large spike in the most recent bin. To avoid a bias in favour of the present field value, we average the dataset by age. Within that set of averages, the interval from 0 to 0.3 Ma is still far more densely sampled than the preceding 300 Ma. We therefore consider the points within this time span as a separate group. Note that the limits of 0 and 0.3 Ma are based solely on the density of samples within that interval and not on any perceived difference in geomagnetic field behaviour. The average VADM within the 0–0.3 Ma interval is $8.4 \pm 3.1 \times 10^{22}$ A m^2. The age distribution of the 0.3–300 Ma averages (figure 5*b*) is closer to uniform, though still imperfect: some bias toward younger samples remains.

The temporal averages and standard deviations of data from the 0.3–300 Ma dataset are shown on figure 5*c*. Taken as a whole, the average VADM of the 0.3–300 Ma dataset is $4.6 \pm 3.2 \times 10^{22}$ A m^2. There appears to be no long-term trend, although the large standard deviation relative to the mean reflects the high short-term variability. Few averages come close to or exceed the 0–0.3 Ma average VADM. In § 3 *b* (ii), we will examine some statistical measures of the difference between the 0–0.3 Ma and 0.3–300 Ma datasets.

Previous authors, beginning with Cox (1968), have predicted an inverse relationship between the Earth's dipole moment and the frequency of polarity reversals. We have plotted an estimate of reversal frequency for the past 160 Ma (C. G. Constable 1999, personal communication) on an inverted scale along with the average estimated

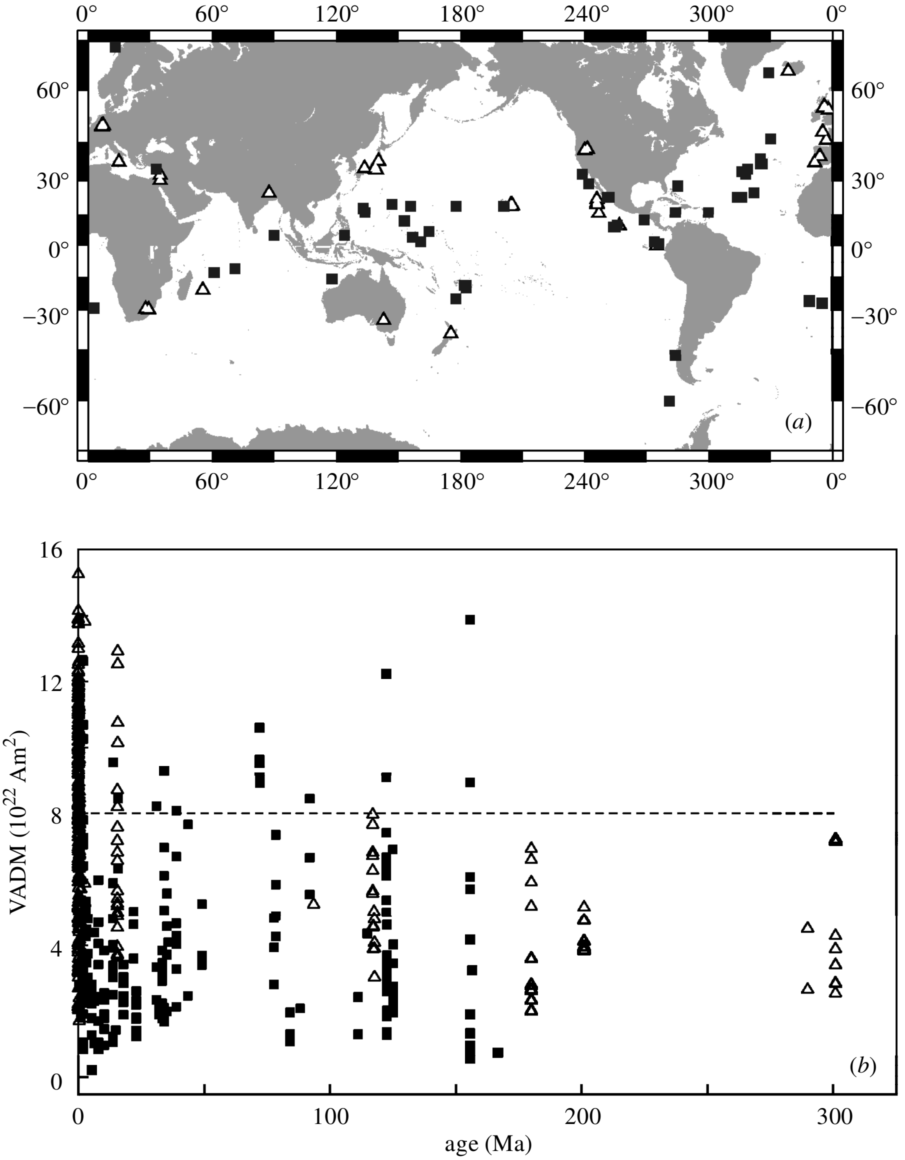

Figure 4. (*a*) Map of locations of the sampling sites of the palaeointensity data compiled in this paper. Squares are for the SBG99 dataset and triangles are the same as in figure 3. (*b*) VADMs of the SBG99 (squares) and PINT99 (triangles) data compiled here.

VADM values in figure 5*c*. Our data are so widely spaced in age that attempting to calculate the coherence of the two signals, for example, would be meaningless. However, we can choose two periods with different reversal frequencies and compare the distribution of VADM estimates between the two. We choose as a division the change in reversal rate from three reversals per million years to nearly two reversals per million years at *ca.* 30 Ma. The VADM estimates from 0.3–30 Ma represent a quickly reversing regime, whereas from 30 to *ca.* 124 Ma (at which point the reversal rate is

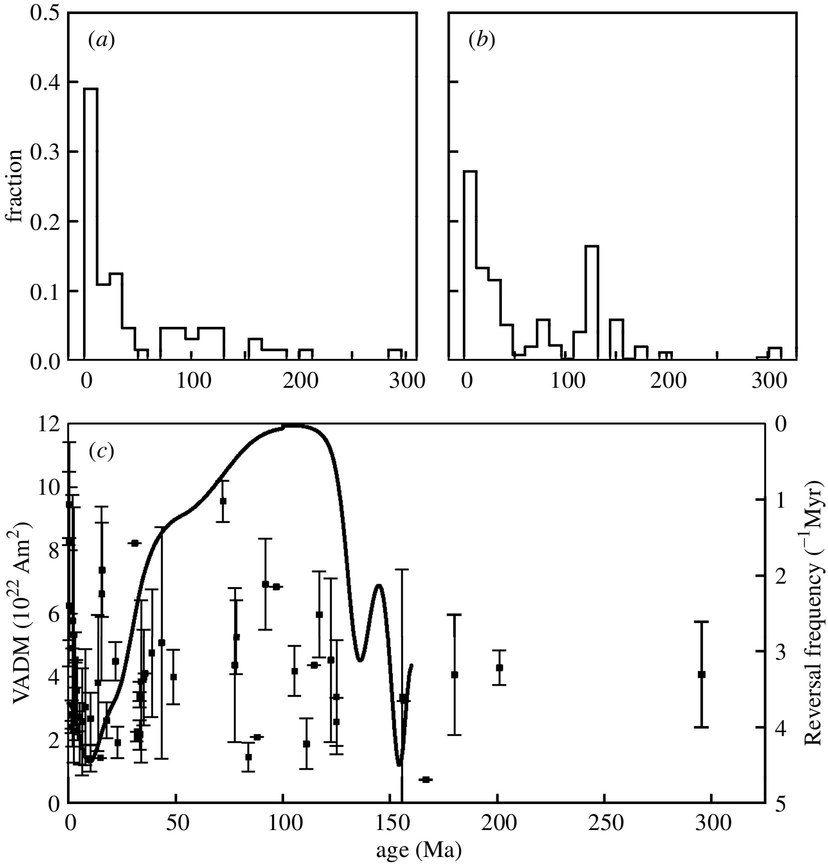

Figure 5. (*a*) Distribution of ages of individual data points in the SBG99/PINT99 combined database. The ages are heavily skewed to the last few hundred thousand years. (*b*) Distribution of ages of data averaged by sampling site, excluding data younger than 0.3 Ma. (*c*) Average VADMs for SBG99/PINT99 data shown as dots with standard deviations as uncertainty bounds. Heavy line is the estimated reversal frequency of Constable (1999, personal communication). We divide the data into categories of 'fast' reversal rate (greater than 3 Myr^{-1}) and 'slow' (less than 3 Myr^{-1}) (see text).

dominated by reversals corresponding to the M-series marine magnetic anomalies) the geomagnetic field reverses less frequently. We will compare the distributions of VADMs from the two periods.

(ii) *Comparison of palaeointensity: reversal rate and palaeointensity*

To compare palaeointensity variations from the quickly and slowly reversing regimes, we consider the data not as sections of a time-series, but rather as populations of points drawn from some underlying distribution (or distributions). We will compare the distribution of VADMs from the fast reversal rate period (0.3–30 Ma) to those from the slow reversal rate period (30–124 Ma). To illustrate the similarity between VADM distributions from these two time-segments, we have constructed approximate cumulative distribution functions (CDFs, figure 6*a*). The VADM esti-

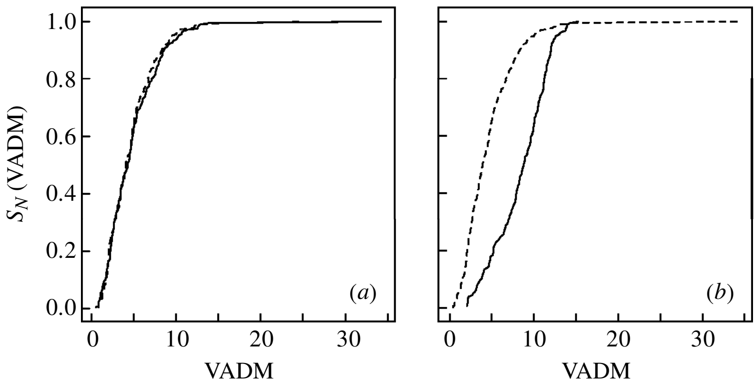

Figure 6. Cumulative distribution functions for the data shown in figure 5. (*a*) VADMs ($\times 10^{22}$ A m^2) from the period of time with a 'fast' reversal rate (see caption for figure 5) are shown as a dashed line and those from a 'slow' time as a solid line. The Kolmogorov–Smirnov statistic d_n and probability P comparing these two datasets are 0.06 and 0.79, respectively. These parameters suggest that two distributions are not significantly different. (*b*) Same as in (*a*) but for VADMs from 0–0.3 Ma (solid line) and 0.3–300 Ma (dashed line). These distributions are significantly different at a very high degree of confidence ($d_n = 0.53$, $P = 3 \times 10^{-29}$).

mates are culled from the combined SBG99 and selected PINT99 datasets mentioned above.

The CDFs of the fast and slow data are strikingly similar: $4.8 \pm 3.5 \times 10^{22}$ A m^2 for the 0.3–30 Ma data and $4.7 \pm 3.0 \times 10^{22}$ A m^2 for the 30–124 Ma data. If one chooses different age limits for these datasets—in particular, if one compares our fast reversal rate dataset with VADM estimates from the Cretaceous Normal Superchron alone—the two datasets remain similar (the average VADM for during the Cretaceous Normal Superchron is $4.9 \pm 2.2 \times 10^{22}$ A m^2).

We have a powerful tool at our disposal for testing whether two datasets were drawn from the same distribution: the Kolmogorov–Smirnov (KS) test (Press *et al*. 1992). This test is non-parametric—it does not require any initial assumptions about the distribution underlying the data. The KS test is based on the statistic d_n, a measure of the maximum deviation between the estimated CDFs of two datasets (S_{N1} and S_{N2}):

$$d_n = \max_{-1 < x < 1} |S_{N1}(x) - S_{N2}(x)|. \tag{3.1}$$

The theoretical distribution of d_n can be used to determine whether the results of the KS test are significant. The probability that the deviation of two datasets, each containing N observations, would be greater than d_n is given by

$$P(D_N < d_n) = 2\sum_{i=1}^{1} (-1)^{i-1} \mathrm{e}^{-2i^2 N d_n^2}. \tag{3.2}$$

A low value of P indicates that it is unlikely that d_n could be the deviation between the CDFs of two sets of observations drawn from the same distribution. We reject the null hypothesis—that the distributions are the same—when $P < 0.05$.

Applying the KS test to the 0.3–30 and 30–124 Ma datasets, we obtain a small value for the deviation ($d_n = 0.062$) and find that the two datasets are similar to within

79% confidence. This is not a resounding confirmation of our initial impression based on the CDFs. However, we cannot reject the hypothesis that the two distributions are the same in this case.

(iii) *Comparison of palaeointensity: most recent data versus older data*

We have also estimated CDFs for the most recent densely sampled (0–0.3 Ma) VADMs and for the VADMs from 0.3 to 300 Ma (figure 6*b*). Note that the CDF of the 0–0.3 Ma dataset is dramatically different from that of the older VADMs. The difference in the CDFs implies not only that the two datasets differ in terms of their mean and variance, which we have already discussed, but that the two datasets differ qualitatively in their distribution. The 0–0.3 Ma data are much more uniformly distributed over the range of VADMs than are the 0.3–300 Ma data. The latter contains considerably fewer data in the lowest and highest ranges of VADM values relative to the mean, whereas such points are common in the young dataset.

When we apply the KS test to determine whether the 0–0.3 Ma dataset is similar to the 0.3–300 Ma data, we obtain a d_n of 0.526 and a significance level of 3.11×10^{-29}. These results indicate that the two datasets do represent significantly different distributions.

(iv) *Justification for selection based on method*

We could make a stronger case for excluding palaeointensity estimates based on technique if we could show that VADMs estimated using full Thellier data are distinctly different from those estimated by other means. We therefore examine data from the PINT99 database which we had excluded from our previous calculations because they were the result of Shaw, Van Zijl, Wilson, ordinary Thellier, or other methods. We focus on data from the past 5 Ma because it is easiest to calculate VADMs for these points (see § 2 *d*). The VADM estimates from the excluded data are plotted along with averages of data which passed our selection criteria in figure 7*a*. VADMs of the excluded data are more widely scattered than are our accepted data. Furthermore, the VADMs of the excluded data appear to be nearly evenly distributed over the past 5 Ma, whereas we have already discussed at length the low VADMs of the accepted data older than 0.3 Ma.

Comparing estimated CDFs of the excluded and included datasets supports our contention that the two datasets are significantly different, although the difference is not apparent over the 0–0.3 Ma time span (figure 7*b*). The CDFs of included and excluded data from 0.3–5 Ma, however, indicate that the excluded data do indeed have a much higher variance (as evidenced by the spread of the CDF along the VADM axis). The excluded data also have a long tail at high values suggesting that the distribution of excluded data is skewed toward these values. The mean of the excluded 0.3–5 Ma data is $7.92 \pm 3.99 \times 10^{22}$ A m^2, close to that of the 0–0.3 Ma excluded data ($8.17 \pm 2.48 \times 10^{22}$ A m^2).

Finally, we use the KS test to compare the data deemed acceptable in this paper with the excluded data. The test strongly suggests that the included and excluded data in the interval 0.3–5 Ma are significantly different ($d_n = 0.299$ with a significance of 4×10^{-5}).

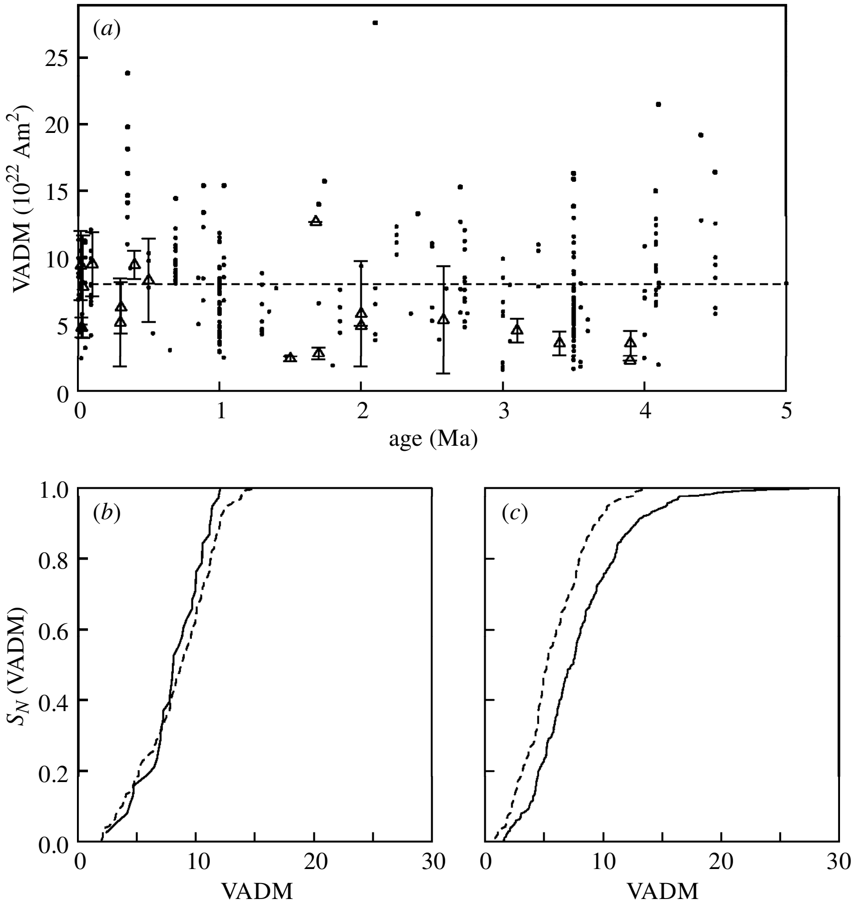

Figure 7. Effect of including less reliable results on the calculation of the mean dipole moment. (*a*) All VADMs from the last 5 Myr from the Montpellier 1999 database. Averages by age of data from SBG99 and PINT99 that meet our minimum criteria for acceptance are shown as triangles and those excluded are shown as dots. (*b*) Cumulative distribution functions (see caption for figure 5), for included (dashed line) and excluded data (solid line) for the period 0–0.3 Myr. Data are in units of 10^{22} A m^2. These two datasets are similar ($d_n = 0.139$, $P = 0.598$) with a mean of about 8.4×10^{22} A m^2. (*c*) Cumulative distribution functions (see caption for figure 5), for included (dashed line) and excluded data (solid line) for the period 0.3–5 Myr. These two datasets are significantly different ($d_n = 0.299$, $P = 4 \times 10^{-5}$) with means of about 5.7×10^{22} A m^2 (included data) and 7.9×10^{22} A m^2 (excluded data).

(v) *Dipole nature of the field*

Our data also allow us to test whether the geomagnetic field has been dominantly dipolar through time. In figure 8*a*, *b*, we present averages by palaeolatitude of estimated palaeofield intensities. We have also calculated what the intensity of the geomagnetic field should be at a range of latitudes based on the average VADM values determined in § 3 *b* (i). The latter is drawn as a heavy black line in figure 8*a*, *b*. With a few exceptions, dipoles based on average VADM values fit both the 0–0.3 Ma and 0.3–300 Ma datasets to within the standard deviation of the palaeofield estimates.

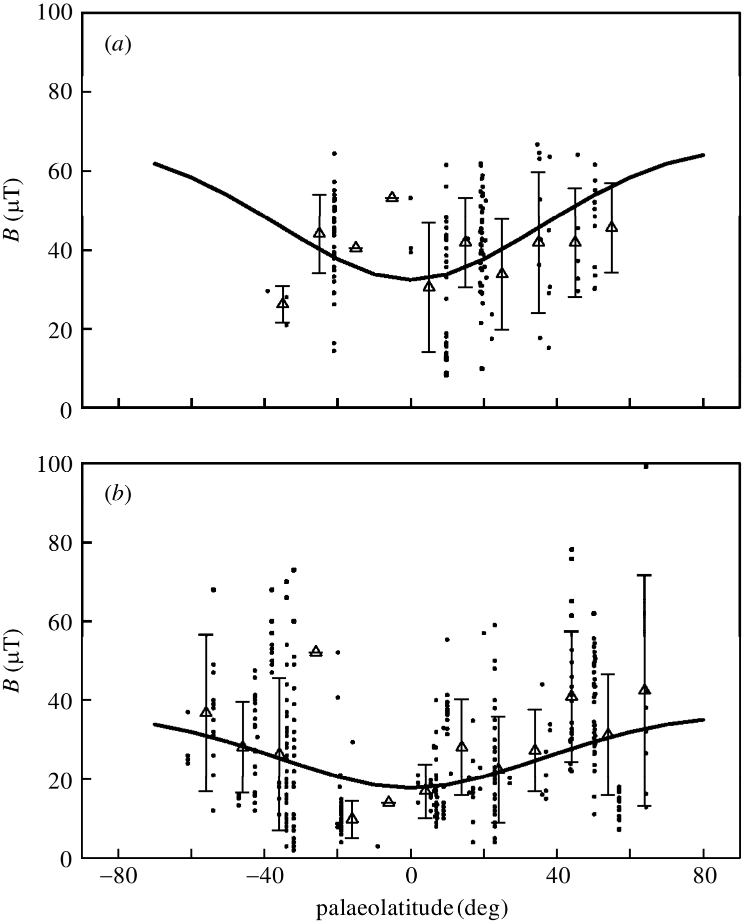

Figure 8. Field values (B) versus palaeolatitude. Individual measurements shown as dots and averages for 10° bins shown as triangles. Solid lines are the latitudinal variations in B expected for the average dipole moments indicated. (a) Data for the period 0–0.3 Ma. Average dipole moment: 8.47×10^{22} A m^2. (b) Data for the period 0.3–300 Ma. Average dipole moment: 4.52×10^{22} A m^2.

The exceptions occur at latitudes where the dataset contains only a few estimates of the ancient field intensity.

4. Discussion

Our most striking observation based on the data collected here is the similarity in mean palaeointensity values between a period with few reversals (30–124 Ma) and a period with a high reversal frequency (0.3–30 Ma). Cox (1968) and other authors since (see Merrill *et al*. 1996) have suggested that reversals are more likely when the geomagnetic field is weak. Our data do not bear this out: over the long term, palaeointensity does not appear to vary with reversal rate.

On the other hand, we do observe a significant difference between shorter-time-scale variations (represented by the 0–0.3 Ma dataset) and longer-term palaeointensity variations (the 0.3–300 Ma data). Previous studies have noted a similar dramatic difference between the intensity of the geomagnetic field in the recent past and that value over geological time (see, for example, Juarez *et al*. 1998; Juarez & Tauxe 2000). Because we re-evaluate much of the data from these studies, our results are not entirely independent of theirs. However, our new submarine basaltic glass data and the reliable palaeointensity estimates from the PINT99 database do confirm their conclusions that the present geomagnetic field is stronger than the long-term average.

From the data presented above, we tentatively conclude that variations on a shorter time-scale (of the order of 10^5 yr) are driven by a fundamentally different process than is the more stable long-term palaeointensity (averaged over *ca.* 100 Myr). We cannot be certain of this because of the poor temporal resolution of the current dataset. Such a conclusion, however, is at variance with the most recent set of results from magnetohydrodynamical modelling of the core. In the models of Glatzmaier *et al.* (1999), behaviour of the geomagnetic field varies drastically with boundary conditions on the outer core—among which, notably, is the thermal structure of the lower mantle. The latter most likely varies over time-scales similar to those of plate tectonics (of the order of 100 Ma). Not only is the recent palaeointensity highly surprising, then, but the similarity between our 0.3–30 and 30–124 Ma palaeointensity datasets is all the more unexpected.

It is important to note that we could not have distinguished between palaeointensity variations over the past 0.3 Ma and longer-term palaeointensity averages if we had uncritically accepted all palaeointensity estimates in the published literature. In particular, methods that involve a single NRM–TRM ratio (such as those of Shaw (1974) and Van Zijl *et al*. (1962)) and that do not involve pTRM checks bias palaeointensity estimates to high values. The resulting VADM values throughout the past are close to the present dipole moment.

The bias toward young samples in both databases may also affect estimates of long-term palaeointensity trends. Because such a large percentage of the VADM estimates are from very young samples (less than 0.3 Ma), an unweighted average of all VADM estimates in either database will be biased toward the present—anomalously high—field intensity.

PHILOSOPHICAL TRANSACTIONS OF THE ROYAL SOCIETY A MATHEMATICAL, PHYSICAL & ENGINEERING SCIENCES

5. Conclusions

(1) We strongly caution against using palaeointensity-estimation methods that do not include multiple temperature steps as well as checks (interspersed among heating steps) for irreversible magnetic behaviour. Methods without such precautions are likely to result in biased estimates of the geomagnetic field.

(2) To first order, the geomagnetic field over the past 300 Ma has been dipolar.

(3) The average virtual axial dipole moment of the Earth, as derived from high-quality palaeointensity estimates, has not changed over hundreds of millions of years. From 0.3 to 300 Ma—throughout nearly all of the period for which we have high-quality palaeointensity estimates—the Earth's average VADM has remained at $4.6 \pm 3.2 \times 10^{22}$ A m^2. This provides an interesting backdrop to conclusions based on the latest generation of geodynamo models (see, for example, Glatzmaier *et al*. 1999), which indicate that mantle convection may

play a large role in outer-core behaviour. It is possible that palaeointensity varies over a much longer time-scale (see Stevenson *et al*. 1983), but we cannot determine that using the present database.

(4) In contrast to the lack of long-term variation in palaeointensity, there may be a great deal of short-term variation within the recent past, which is the most densely sampled. Our 0–0.3 Ma dataset indicates an above-average VADM of $8.47 \pm 3.10 \times 10^{22}$ A m^2. We cannot say with certainty whether this is representative of short-term variation in the past—sampling density is uneven at best over the past 300 Ma—but we are convinced that the distribution of palaeointensity estimates over the past 0.3 Ma does not reflect long-term palaeointensity variations.

The authors thank Cathy Constable, Jeff Gee, Steve Cande and Andrew Newell for insightful comments. Thomas Pick and Teresa Juarez kindly provided basaltic glass datasets for use in this paper. We are especially grateful to Steven Di Donna for performing many of the analyses that went into the SBG99 dataset. This work was performed while one of the authors (P.A.S.) held a JOI/USSAC Ocean Drilling Fellowship. P.A.S. was also funded by NSF EAR 9526533.

References

Berggren, W., Kent, D. & Flynn, J. J. 1985*a* Jurassic to Paleogene. Part 2. Paleogene geochronology and chronostratigraphy. In *The chronology of the geological record* (ed. N. Snelling), pp. 141–195. Oxford: Blackwell.

Berggren, W., Kent, D. & Van Couvering, J. 1985*b* The Neogene. Part 2. Neogene geochronology and chronostratigraphy. In *The chronology of the geological record* (ed. N. Snelling), pp. 211–260. Oxford: Blackwell.

Cande, S. & Kent, D. 1995 Revised calibration of the geomagnetic polarity timescale for the late Cretaceous and Cenozoic. *J. Geophys. Res.* **100**, 6093–6095.

Castillo, P., Pringle, M. & Carlson, R. 1994 East Mariana Basin tholeiites: Cretaceous intraplate basalts or rift basalts related to the Ontong Java plume? *Earth Planet. Sci. Lett.* **123**, 139–154.

Coe, R. S. 1967 The determination of paleo-intensities of the Earth's magnetic field with emphasis on mechanisms that could cause non-ideal behavior in Thellier's method. *J. Geomagn. Geoelectr.* **19**, 157–178.

Coe, R. S., Grommé, S. & Mankinen, E. A. 1978 Geomagnetic paleointensities from radiocarbon-dated lava flows on Hawaii and the question of the Pacific nondipole low. *J. Geophys. Res.* **83**, 1740–1756.

Cox, A. 1968 Lengths of geomagnetic polarity intervals. *J. Geophys. Res.* **73**, 3247–3260.

Dziewonski, A. (and 27 others) 1991 *Proceedings of the Ocean Drilling Program, Initial Reports*, vol. 136. College Station, TX: Ocean Drilling Program.

Forsythe, R. D. (and 31 others) 1995 Data report: ^{40}Ar/^{39}Ar and additional Paleontologic age constraints, Site 862, Taitao Ridge. In *Proceedings of the Ocean Drilling Program, Scientific Results* (ed. S. D. Lewis), vol. 141, pp. 421–426. College Station, TX: Ocean Drilling Program.

Glatzmaier, G. A., Coe, R. S., Hongre, L. & Roberts, P. H. 1999 The role of the Earth's mantle in controlling the frequency of geomagnetic reversals. *Nature* **401**, 885–890.

Goguitchaichvili, A., Prévot, M. & Camps, P. 1999 No evidence for strong fields during the R3–N3 Icelandic geomagnetic reversal. *Earth Planet. Sci. Lett.* **167**, 15–34.

Goldstein, S. J. (and 30 others) 1995 Uranium-series chronology of subsurface basalts, 9°31′ N East Pacific Rise. In *Proceedings of the Ocean Drilling Program, Scientific Results* (ed. M. A. Storms), vol. 142, pp. 37–39. College Station, TX: Ocean Drilling Program.

Harland, W. B., Armstrong, R. L., Cox, A. V., Craig, L. E., Smith, A. G. & Smith, D. G. 1989 *A geologic time scale*. Cambridge University Press.

Juarez, T. & Tauxe, L. 2000 The average intensity of the time-averaged geomagnetic field: the past five million years. *Earth Planet. Sci. Lett.* **170**, 169–180.

Juarez, M., Tauxe, L., Gee, J. & Pick, T. 1998 The intensity of the Earth's magnetic field over the past 160 millions years. *Nature* **394**, 878–881.

Kirschvink, J. L. 1980 The least-squares line and plane and the analysis of paleomagnetic data. *Geophys. Jl R. Astr. Soc.* **62**, 699–718.

Kono, M. 1978 Reliability of paleointensity methods using alternating field demagnetization and anhysteric remanence. *Geophys. Jl R. Astr. Soc.* **54**, 241–261.

Lee, T.-Y. & Lawver, L. 1995 Cenozoic plate reconstruction of Southeast Asia. *Tectonophys.* **251**, 85–138.

Mahoney, J., Storey, M., Duncan, R. A., Spencer, K. & Pringle, M. 1993 Geochemistry and age of the Ontong–Java Plateau. In *The Mesozoic Pacific: geology, tectonics and volcanism* (ed. M. Pringle, W. Sager, W. Sliter & S. Stein), ch. 13, pp. 233–262. Washington, DC: AGU.

Merrill, R., McElhinny, M. & McFadden, P. 1996 *Paleomagnetism, the core and the deep mantle*. Academic.

Mueller, R., Royer, J.-Y. & Lawver, L. 1993 Revised plate motions relative to the hotspots from combined Atlantic and Indian Ocean hotspot tracks. *Geology* **21**, 275–278.

Nagata, T., Arai, Y. & Momose, K. 1963 Secular variation of the geomagnetic total force during the last 5000 years. *J. Geophys. Res.* **68**, 5277–5282.

Néel, L. 1949 Théorie du traînage magnétique des ferromagnétiques en grains fins avec applications aux terres cuites. *Ann. Géophys.* **5**, 99–136.

Perrin, M. & Shcherbakov, V. 1997 Paleointensity of the Earth's magnetic field for the past 400 Ma: evidence for a dipole structure during the Mesozoic low. *J. Geomag. Geoelectr.* **49**, 601–614.

Perrin, M., Schnepp, E. & Shcherbakov, V. 1998 Paleointensity database updated. *Eos* **79**, 198.

Pick, T. & Tauxe, L. 1993*a* Geomagnetic paleointensities during the Cretaceous normal superchron measured using submarine basaltic glass. *Nature* **366**, 129–139.

Pick, T. & Tauxe, L. 1993*b* Holocene paleointensities: Thellier experiments on submarine basaltic glass from the East Pacific Rise. *J. Geophys. Res.* **98**, 17 949–17 964.

Pick, T. & Tauxe, L. 1994 Characteristics of magnetite in submarine basaltic glass. *Geophys. Jl Int.* **119**, 116–128.

Press, W., Teukolsky, S., Vetterling, W. & Flannery, B. 1992 *Numerical recipes in C*, 2nd edn. Cambridge University Press.

Prévot, M., Mankinen, E., Coe, R. & Grommé, C. 1985 The Steens Mountain (Oregon) geomagnetic polarity transition. 2. Field intensity variations and discussion of reversal models. *J. Geophys. Res* **90**, 10 417–10 448.

Rolph, T. & Shaw, J. 1985 A new method of paleofield magnitude correction for thermally altered samples and its application to lower carboniferous lavas. *Geophys. Jl R. Astr. Soc.* **80**, 773–781.

Shaw, J. 1974 A new method of determining the magnitude of the paleomagnetic field: application to five historic lavas and five archaeological samples. *Geophys. Jl R. Astr. Soc.* **39**, 133–141.

Sigurdsson, H. (and 27 others) 1996 *Proceedings of the Ocean Drilling Program, Initial Reports*, vol. 165. College Station, TX: Ocean Drilling Program.

Stevenson, D., Spohn, T. & Schubert, G. 1983 Magnetism and thermal evolution of the terrestrial planets. *Icarus* **54**, 466–489.

Tanaka, H., Kono, M. & Uchimura, H. 1995 Some global features of paleointensity in geological time. *Geophys. Jl Int.* **120**, 97–102.

Thellier, E. & Thellier, O. 1959 Sur l'intensité du champ magnétique terrestre dans le passé historique et géologique. *Ann. Geophys.* **15**, 285–378.

Van der Voo, R. 1993 *Paleomagnetism of the Atlantic, Tethys and Iapetus Oceans*. Cambridge University Press.

Van Zijl, J., Graham, K. & Hales, A. 1962 The paleomagnetism of Stormberg lavas. II. The behaviour of the magnetic field during a reversal. *Geophys. Jl Lond.* **7**, 169–181.

Wallick, B. & Steiner, M. 1992*a* Paleomagnetic and rock magnetic properties of Jurassic quiet zone basalts, hole 801C. In *Proceedings of the Ocean Drilling Program, Scientific Results* (ed. R. Larson *et al.*), pp. 455–470. College Station, TX: Ocean Drilling Program.

Wallick, B. & Steiner, M. 1992*b* Paleomagnetism of Cretaceous basalts from the East Mariana Basin, Western Pacific Ocean. In *Proceedings of the Ocean Drilling Program, Scientific Results* (ed. R. Larson *et al.*), pp. 447–454. College Station, TX: Ocean Drilling Program.

Wilson, R. 1961 Paleomagnetism in Northern Ireland. I. The thermal demagnetization of natural magnetic moments in rocks. *Geophys. Jl Lond.* **5**, 45–58.

Yan, C. & Kroenke, L. 1993 A plate tectonic reconstruction of the Southwest Pacific 0–100 Ma. In *Proceedings of the Ocean Drilling Program, Scientific Results* (ed. W. Berger *et al.*), pp. 697–709. College Station, TX: Ocean Drilling Program.